IRAQI JOURNAL OF APPLIED PHYSICS
Vol. 22, No. 2, April-June 2026, pp. 243-248

Maha M. Awsaj *
Luma A. Jassim
Anwar A. Hameed

Department of Chemistry,
College of Science,
University of Tikrit,
Salah Alden, IRAQ
Corresponding author email:
maha.m.awsaj@tu.edu.iq

Kinetic, Thermodynamic Study of Phenol Red Dye Adsorption Using CuO-PVC Nanocomposite

The PVC-CuO nanocomposite has been synthesized and characterized by X-ray diffraction (XRD) and field-emission scanning electron microscopy (FE-SEM). It served as an adsorbent for the adsorption of phenol red. The influence of several parameters, the adsorbent eliminated 94.47% of phenol red under optimal conditions: adsorbent dose of 0.01 g, contact time of 45 minutes, starting concentration of 50 mg/L, temperature of 298 K (25°C), and pH of 7. Experimental data was matched by the pseudo second-order kinetics. The free energy values at temperatures of 293, 298, 303, and 313 K were determined to be -2.289, -2.452, -3.0154 kJ/mole, respectively. Negative free energy values signify that the adsorption of phenol red is spontaneous. The results for enthalpy and entropy change were 42.235 kJ/mole and 61.342 kJ/mole, respectively. Adsorption process was endothermic due to the positive enthalpy value. Adsorption exhibited an increase in randomness at the PVC-CuO nanocomposite-phenol interface, as indicated by the positive value of the entropy change obtained.

Keyword: Nanocomposites; Dye adsorption; Thermodynamics; Phenol red dye
Received: 30 June 2025; Revised: 5 October 2025; Accepted: 12 October; Published: 1 April 2026

1. Introduction

The primary pollutants in wastewater bodies are organic dyes, which are poisonous, carcinogenic, and detrimental to both human and aquatic life [1]. Dyes are primarily composed of many aromatic compounds that exhibit significant stability when exposed to oxidants or elevated temperatures [2]. The removal of hazardous dyes, which are challenging to treat, has been the subject of extensive study aimed at developing cost-effective and efficient solutions. Despite numerous proposed methods for dye removal, adsorption processes remain the most interesting strategies due to their simplicity, cost-effectiveness, and high efficiency [3]. The adsorption technique has demonstrated high efficacy in eliminating organophosphates from wastewater. Adsorption is a fundamental surface phenomenon in which contaminants are selectively extracted from an aqueous solution by adhering the solute (adsorbate) to a solid surface (adsorbent) [4]. Sometimes the process of adsorption is reversible due to presence of weak van der walls bonds between adsorbent and adsorbate [5].

Activated carbons, recognized for their superior adsorption capacity, are the most extensively studied adsorbents for the removal of organic compounds from wastewater. Although activated carbons are often regarded as effective adsorbents, their application is constrained by the high costs associated with manufacture and regeneration. Consequently, innovative materials, including nanomaterials, have been created and are actively employed in water treatment to purify water by eliminating pollutants such as heavy metals, harmful organic dyes, greasy waste, and numerous industrial and agricultural contaminants. Nanomaterials, commonly known as nanoparticles, are particles that range in size from 1 to 100 nanometers. Alongside wastewater treatment, contemporary research emphasizes the advancement of nanomaterials for optical data storage, sensors, and resilient, lightweight construction materials. Despite both nanoparticles and activated carbon possessing significantly high surface areas, some nanomaterials offer two primary advantages as adsorbents: they can be manufactured more quickly and at a reduced cost, and less quantities are necessary for the effective removal of contaminants [10]. Consequently, nanoparticles are anticipated to be more cost-effective than activated carbon for adsorption applications [11]. Nonetheless, there exists a paucity of research concerning the composites of metal oxides with polymers as adsorbents. Surface modification of metal oxides with polymers occurs via many mechanisms, including electrostatic, hydrophobic, and covalent bonding, with hydrogen bonding seen as a predominant method.

Polyvinyl chloride (PVC) is extensively utilized in electrical cables, synthetic leather, colored textiles, healthcare applications, construction, piping, household items, and fashion, owing to its exceptional characteristics, including weather resistance, low maintenance, cost efficiency, flame retardance, non-toxicity, malleability, and biological activity [12]. Additionally, PVC can undergo structural modification through the removal and nucleophilic substitution of chlorine atoms [13]. Consequently, chemically modified PVC may be examined as a viable adsorbent for dye removal [14]. Metal oxides modified by PVC have garnered significant interest for advantageous uses in adsorption. Similarly, PVC has been identified as a good choice for effectively enhancing the proportion of active sites, exposed surface area, functional groups, and porosity of metal oxide

nanosheets by reducing their thickness [15]. Copper oxide (CuO), often known as cupric oxide, is a semiconducting chemical characterized by a monoclinic structure. CuO has garnered significant interest as the most elementary member of the copper compound family, demonstrating a variety of potentially advantageous physical features, including high-temperature superconductivity, electron correlation phenomena, and spin dynamics [16], As a significant p-type semiconductor, CuO has numerous uses, including gas sensors, catalysis, batteries, high-temperature superconductors, solar energy conversion, and field-emission emitters. In the realm of energy conservation, energy transfer fluids infused with CuO nanoparticles can augment fluid viscosity and improve thermal conductivity [17]. CuO crystal formations exhibit a low band gap, imparting valuable photocatalytic and photovoltaic features, along with photoconductive capabilities [18]. The application of copper ions on the surface of nanocomposites can augment electrostatic interactions [19] and donor-acceptor systems including the dye molecules [20,21]. The synthesis of polymer nanocomposites, taking into account the aforementioned features, provides an effective approach to address the challenges posed by some nanofillers in environmental applications, including separation and reuse [22].

This study involved the synthesis of copper oxide nanoparticles (CuO NPs) doped into polyvinyl chloride (PVC) for the removal of phenol red (Ph.R) dye. The impact of several factors, including adsorbent dose, pH, and temperature, on the adsorption process was examined. The Langmuir, Freundlich, and Tempkin isotherms were utilized to describe the adsorption of Ph.R dye on CuO NPs doped with PVC. Additionally, pseudo-first and pseudo-second-order kinetic models were employed to evaluate the adsorption mechanism.

2. Experimental Part

Raw materials include phenol red, HCl, NaCl, Na_2CO_3, NaOH, $Cu(NO_3)_2{\cdot}6H_2O$, adsorbent surface (polyvinyl chloride (PVC) + CuONPs), adsorbent surface (phenol red) from Fluka and BDH suppliers.

A dye (Ph.R) was prepared at a concentration of 50 mg/L by dissolving 50 mg in 1000 mL of distilled water, and a series of dilute solutions were prepared [23].

The sol-gel process has been employed to synthesize CuO NPs that are incorporated into the PVC matrix [24]. Commencing with 30 ml of Triton X-100, 19.275 g of $Cu(NO_3)_2{\cdot}6H_2O$ was dissolved in 50 ml of distilled water and mixed at 27°C. The solution was subsequently heated to 123°C in the furnace to obtain the gel precursor. The gel fine powder was calcined at 600°C for 2 hours at a rate of 5 °C/min in air to produce black CuO nanopowder. The PVC/CuONPs films with varying concentrations of CuO NPs (0, 2.5, 5.0, 10.0, and 15.0 wt.%) are synthesized as follows: 2 g of extra pure PVC powder, with a density of 1.4 g/ml at 25°C, is dissolved in 30 ml of tetrahydrofuran (THF) for 60 min. Different ratios of CuO NPs are incorporated into the aforementioned solution with continuous agitation for 60 min. The solution is ultimately transferred to a glass dish and allowed to dry in the air to obtain the desired films.

3. Results and discussion

XRD analysis was performed to study the crystallinity nature of the PVC/CuONPs nanocomposite. The XRD pattern in Fig. (1) reveals that the addition of PVC fillers to the CuO NPs matrix significantly increased the range of the amorphous region (i.e., the intensity of the XRD crystal peak decreased).

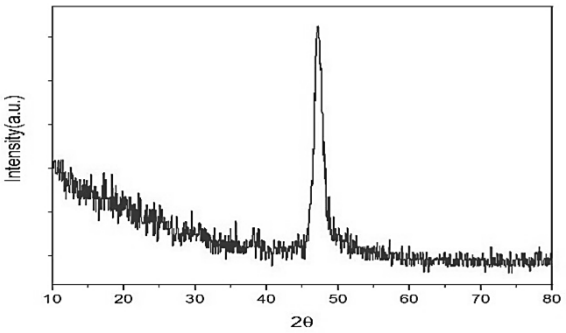

Fig. (1) XRD pattern of PVC\CuONPs nanocomposite

The XRD pattern demonstrates the amorphous characteristics of PVC and its distinctive broad peak at 20° to 24°. The film doped with CuO NPs demonstrated the crystallization of CuO NPs, exhibiting crystalline peaks at 2θ approximately 35°, 44°, 50°, and 72° [25].

The surface morphology of the synthesized PVC/CuONPs nanocomposite for basic dye removal is displayed in Fig. (2). The PVC film prepared from PVC waste is characterized by the presence of a thick and dense surface, which increases the presence of mesoporous and microporous (nanoscale range). Figure (2) indicated that the PVC/CuONPs nanocomposite have tube shape with diameter of 392.7 nm. Also, the distribution is very smooth within a rough surface.

The pH is a critical factor influencing the adsorption capacity of phenol red on the surface of modified PVC/CuONPs nanocomposite. Variations in pH alter the dissociation of functional groups on the adsorbent, thus impacting its affinity for the adsorbate. The trials were performed with pH variations ranging from 3 to 11 and phenol concentrations of 50 mg/L. The dosage, duration, and temperature were constant at 10 g/L, 60 min., and 25°C. Table (1) illustrates that elimination of phenol red dye increases occurs with pH levels ranging from 3 to 7. Beyond pH=8, the elimination significantly diminished [26].

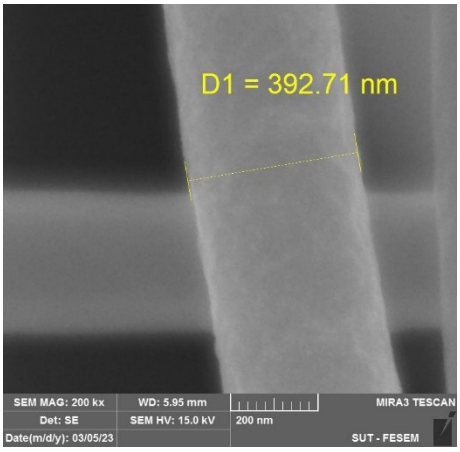

Fig. (2) FE-SEM image of the synthesized PVC/CuONPs nanocomposite

Table (1) Effect of the pH function on the adsorption percentage using PVC\CuONPs prepared on Ph.R dye

pH	3	5	7	9	11
Absorbance Percentage (%)	94.45	89.45	86.65	71.35	61.4

The highest clearance rate of 94.42% was observed at pH 3, which diminished as pH increased to 11. The adsorption capability progressively diminished with rising pH levels. At low pH, the heightened degree of protonation on the adsorbent surface enhances diffusion, hence facilitating enhanced adsorption by electrostatic attraction. The heightened adsorption of phenol red at low pH resulted from the surplus H^+ ions, which augment the dye's adherence to the adsorbent's sites.

The impact of adsorbent dosage on the removal of phenol red dye using PVC/CuONPs nanocomposite was investigated by increasing the dosage from 0.01 to 0.1 g, with a phenol red dye concentration of 50 mg/L, a shaking duration of 60 min., a constant pH of 7 and ambient temperature (25°C). The results were plotted as the percentage clearance and quantity absorbed of phenol red dye against the adsorbent dose, as shown in table (2). The percentage removal of Ph.R dye rises from 0.01 to 0.07 g, and then declines with increasing adsorbent dosage. The higher doses did not yield a significant enhancement in the elimination [27]. Therefore, the optimal dose of the adsorbent for Ph.R dye elimination was determined to be 0.01 g. The adsorption capability diminishes as the adsorbent dosage increases.

Table (2) Effect of adsorbent dose at 50 ml of Ph.R dye, 10 m/L initial concentration of Ph.R dye, 60 min., pH of 7 and room temperature (25°C)

Weight of Adsorbent	0.01	0.013	0.025	0.07	0.1
Absorbance Percentage (%)	87.55	86.55	89.6	91.25	90.2

The batch tests were performed with variations in time (5-60 min) and Ph.R dye content (50 mg/L). The pH, dosage, and temperature were kept constant at 7, 0.01 g/L, and 25°C, respectively. The removal was initially expedited due to the availability of vacant sites on the adsorbent. Simultaneously, the oxide of the adsorbent participated in the adsorption process, while the oxygenated surface of the adsorbent enhanced adsorption by hydrogen bonding with the hydroxyl surface of Ph.R dye. After 45 min, equilibrium was reached; irrespective of Ph.R dye content, the adsorption sites became saturated, rendering further adsorption impossible [28].

The temperature is crucial in the adsorption phenomena as it markedly influences the adsorption capacity of the adsorbent. The effect of temperature on the adsorption of Ph.R dye by all produced films was investigated at a constant dye concentration of 50 mg/L and an adsorbent dose of 10 mg of PVC/CuONPs, within a temperature range of 20-40°C, with increments of 5°C over an equilibrium period of 60 min.

Table (3) Effect of the temperature on the adsorption percentage using PVC\CuONPs prepared on Ph.R dye

Temperature (K)	293	298	303	313
Absorbance Percentage (%)	89.5	89.85	92.8	95.3

The data acquired were illustrated as percentage elimination and quantity absorbed in relation to temperature, as shown in table (2). The quantity adsorbed and percentage clearance of Ph.R dye were found to rise as the temperature rose from 293 to 313K (20 to 50°C). Comparable findings were previously by certain researchers [29].

Thermodynamic parameters such as standard free energy change (ΔG^0), standard enthalpy change (ΔH) and standard entropy change (ΔS) can be calculated using the following equation:

$$\Delta G^0 = - RT \ln Kc \quad (1)$$

$$\Delta G^0 = \Delta H - T\Delta S \quad (2)$$

$$\ln K = \Delta S/R - \Delta H/RT \quad (3)$$

$$K_c = q_e/C_e \quad (4)$$

Table (4) Values of ΔG^0, ΔH^0 and ΔS^0

T	ΔG^0 (kJ\m)	ΔH^0 (kJ\m)	ΔS^0 (kJ\M. K)
293	-2.289		
298	-2.452	42.235	61.342
303	-3.0154		
313	-3.5599		

The graph of $\ln(K_c)$ versus 1/T establishes the values of ΔG^0, ΔS^0, and ΔH^0, as detailed in table (6). The negative values of ΔG^0 indicate that the adsorption process was spontaneous. The positive ΔH^0 indicated an endothermic process. The positive ΔS^0 indicated an increased level of disorder during the adsorption process.

The pseudo-first order equation can be written as follows [30]:

$$\text{Ln}(q_e - q_t) = \text{Ln}(q_e) - K_1 t \backslash 2.303 \quad (5)$$

where q_e is the number of selected compounds adsorbed at equilibrium (mg/g), q_t is the number of selected compounds adsorbed at time t (mg/g), K_1 (1/min) is the pseudo-first order rate constant

The pseudo-second order model is as the following equation [31]:

$$t \backslash q = 1/(K_2 . q_{e2}) + 1/q_e . t \quad (6)$$

where K_2 (g/mg.min) denotes the rate constant of the second-order equation

The parameters of the pseudo-first-order and pseudo-second-order kinetic models are presented in figures (3) and (4). Analysis of the R2 value and the discrepancy in q_e derived from two models relative to the empirical q_e revealed that the pseudo-second-order model exhibited superior goodness of fit to the experimental data compared to the pseudo-first-order model.

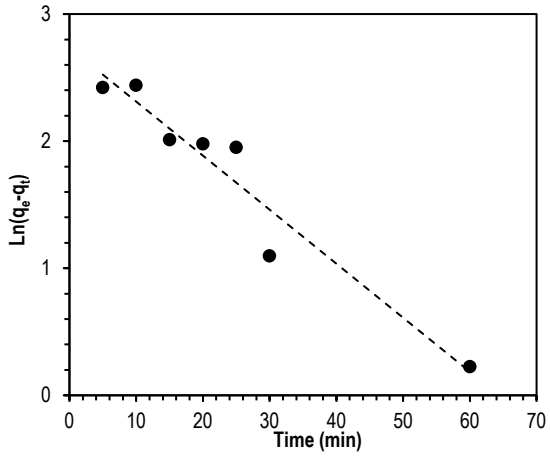

Fig. (3) Pseudo-first-order kinetics

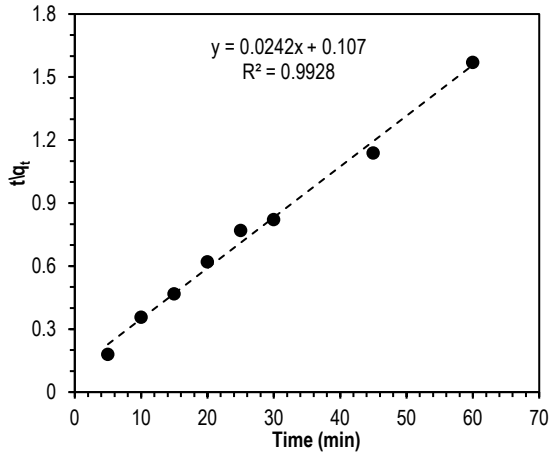

Fig. (4) Pseudo-second-order kinetics

The adsorption data obtained was fitted to various isotherm models in order to find out the nature of adsorption. The linear form of Temkin equation is given below [32]:

$$q_{ads} = BT\ \text{Ln}(KT) + BT\ \text{Ln}(C_{eq}) \quad (7)$$

The Temkin isotherm equation posits that the heat of adsorption for all molecules in the layer diminishes linearly with coverage, attributable to adsorbent–adsorbate interactions, and that the adsorption process is defined by a uniform distribution of binding energies, up to a certain maximum binding energy. The plot of q_{ads} (mg/g) against $\text{Ln}(C_{eq})$ (mg/L) yields a linear relationship characterized by a slope of BT (mg/g) and an intercept of BT Ln(KT) (L/g), as illustrated in Fig. (5). Here, BT represents the heat of adsorption, with its value derived from the graph, while KT denotes the binding energy between the adsorbent and adsorbate, also calculated from the graph, as detailed in table (5).

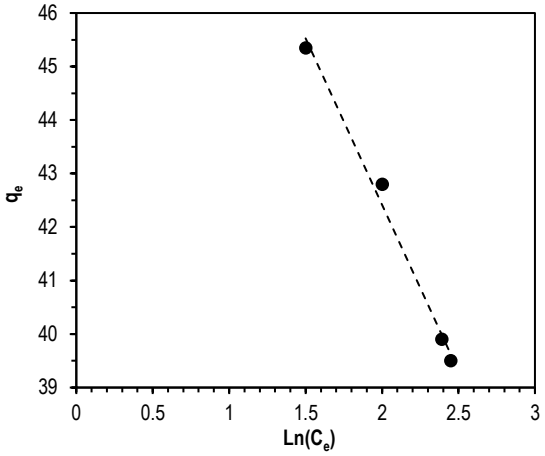

Fig. (5) Adsorption data according to Temkin isotherm model

Table (5) Temkin model parameters

Dye	K_T	BT (L/mg)	R
Ph.R	0.880	56.66	0.98

The linear form of Freundlich isotherm is given below [33]:

$$\text{Ln}(q_{ads}) = \text{Ln}(K_F) + 1 \backslash n \text{Ln}(C_{eq}) \quad (8)$$

Plot of $\text{Ln}(q_{ads})$ (mg/g) versus $\text{Ln}(C_{eq})$ (mg/L) will give 1/n as slope and $\text{Ln}(K_F)$ (mg/g) as an intercept and its value calculated from the graph in Fig. (6) and shown in table (6), where K_F is a constant showing degree of adsorption and n is the heterogeneous factor and is related to intensity of adsorption.

Table (6) Freundlich model parameters

Dye	K_F	n	R
Ph.R	0.832	0.2433	0.994

The Langmuir model is a prevalent two-parameter isotherm utilized to assess adsorption on various adsorbents; according to this model, adsorption energy remains constant regardless of surface coverage. The

Langmuir model posits that all adsorption sites are homogeneous and each site can accommodate just one species. The adsorption process occurs in a monolayer [34]. The Langmuir isotherm equation is stated as follows:

$$q_e = (q_m K_L C_e) / (1 + K_L C_e) \quad (9)$$

In this equation, q_e, C_e, q_m, and K_L (L/mg) represent the quantity of adsorbed phenol red dye per specified mass of PVC/CuO nano-adsorbent (mg/g), the equilibrium concentration of the dye solution (mg/L), the maximum adsorption capacity (mg/g), and the Langmuir equilibrium constant, respectively. Figure (7) illustrates the Langmuir isotherm graph depicting the adsorption of dye onto the adsorbent. The parameters and correlation coefficients derived from the Langmuir equation are presented in table (7), indicating that the Langmuir model most accurately represents the experimental data.

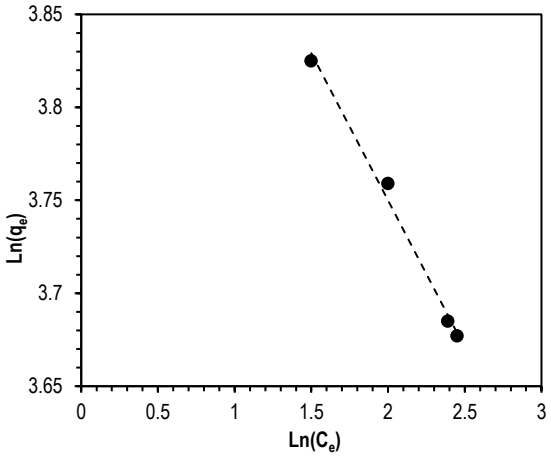

Fig. (6) Adsorption data according to Freundlich isotherm model

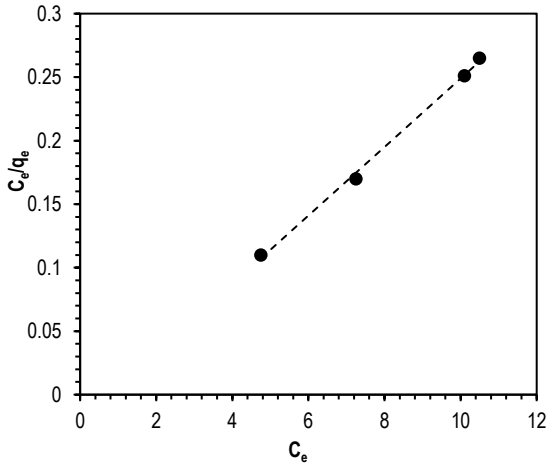

Fig. (7) Adsorption data according to Langmuir isotherm model

Table (7) Langmuir model parameters

Dye	K_L	B	R
Ph.R	1.090	32.78	0.9991

4. Conclusion

The research demonstrated the efficacy of PVC/CuONPs as an effective and cost-efficient adsorbent (92%) for the removal of phenol red dye from aqueous solutions within a short duration (≤45 min). The Langmuir isotherm can effectively characterize adsorption isotherms in comparison to alternative models. The kinetic study results of phenol red dye on PVC/CuONPs demonstrated that adsorption adheres to the pseudo-second-order model, following evaluations based on both the pseudo-first-order and pseudo-second-order models. Variations in activation enthalpy (ΔH^0 = 42.2 kJ/mol), free energy of adsorption (ΔG^0 = -2.45), and entropy (ΔS^0 = 61.43) indicate the spontaneous and endothermic nature of the adsorption process.

References

[1] S. Mishra et al., "Cobalt ferrite nanoparticles prepared by microwave hydrothermal synthesis and adsorption efficiency for organic dyes: Isotherms, thermodynamics and kinetic studies", *Adv. Powder Technol.*, 31(11) (2020) 4552-4562.

[2] T. Van Pham et al., "Adsorption behavior of Congo red dye from aqueous solutions onto exfoliated graphite as an adsorbent: kinetic and isotherm studies", *Mater. Today Proc.*, 18 (2019) 4449-4457.

[3] M. Hasanzadeh, A. Simchi and H.S. Far, "Nanoporous composites of activated carbon-metal organic frameworks for organic dye adsorption: Synthesis, adsorption mechanism and kinetics studies", *J. Ind. Eng. Chem.*, 81 (2020) 405-414.

[4] A.M. Awad et al., "Adsorption of organic pollutants by nanomaterial-based adsorbents: An overview", *J. Mol. Liq.*, 301 (2020) 112335.

[5] S. Hussain et al., "Adsorption, kinetics and thermodynamics studies of methyl orange dye sequestration through chitosan composites films", *Int. J. Biol. Macromol.*, 168 (2021) 383-394.

[6] L. Soldatkina and M. Yanar, "Equilibrium, kinetic, and thermodynamic studies of cationic dyes adsorption on corn stalks modified by citric acid", *Colloids Interfaces*, 5(4) (2021) 52.

[7] W.S. Choi and H.J. Lee, "Nanostructured materials for water purification: Adsorption of heavy metal ions and organic dyes", *Polymers*, 14(11) (2022) 2183.

[8] A. Malshe and D. Deshpande, "Nano and microscale surface and sub-surface modifications induced in optical materials by femtosecond laser machining", *J. Mater. Process. Technol.*, 149(1-3) (2004) 585-590.

[9] T. Okada and J. Suehiro, "Synthesis of nano-structured materials by laser-ablation and their application to sensors", *Appl. Surf. Sci.*, 253(19) (2007) 7840-7847.

[10] Y.H. Chen, "Synthesis, characterization and dye adsorption of ilmenite nanoparticles", *J. Non-Cryst. Solids*, 357(1) (2011) 136-139.
[11] K.B. Tan et al., "Adsorption of dyes by nanomaterials: recent developments and adsorption mechanisms", *Separ. Purif. Technol.*, 150 (2015) 229-242.
[12] C. Zhang et al., "Synthesis and Zn (II) modification of hierarchical porous carbon materials from petroleum pitch for effective adsorption of organic dyes", *Chemosphere*, 216 (2019) 379-386.
[13] H.M.A. Ali et al., "Chemically modified polyvinyl chloride for removal of thionine dye (Lauth's violet)", *Materials*, 10(11) (2017) 1298.
[14] M. Landarani, M. Arab Chamjangali and B. Bahramian, "Preparation and characterization of a novel chemically modified PVC adsorbent for methyl orange removal: optimization, and study of isotherm, kinetics, and thermodynamics of adsorption process", *Water Air Soil Pollut.*, 231 (2020) 1-17.
[15] T. Saeed et al., "Comparative study for removal of cationic dye from aqueous solutions by manganese oxide and manganese oxide composite", *Int. J. Environ. Sci. Technol.*, 18 (2021) 659-672.
[16] R.J. Cava, "Structural chemistry and the local charge picture of copper oxide superconductors", *Science*, 247(4943) (1990) 656-662.
[17] K.Y. Kwak and C.Y. Kim, "Viscosity and thermal conductivity of copper oxide nanofluid dispersed in ethylene glycol", *Korea-Aust Rheol J.*, 17(2) (2005) 35-40.
[18] G. Ren et al., "Characterisation of copper oxide nanoparticles for antimicrobial applications", *Int. J. Antimicrob. Agents.*, 33(6) (2009) 587-590.
[19] D. Bingöl et al., "Analysis of adsorption of reactive azo dye onto $CuCl_2$ doped polyaniline using Box–Behnken design approach", *Synth. Met.*, 162(17-18) (2012) 1566-1571.
[20] S. Dashamiri et al., "Multi-response optimization of ultrasound assisted competitive adsorption of dyes onto $Cu(OH)_2$-nanoparticle loaded activated carbon: central composite design", *Ultrason. Sonochem.*, 34 (2017) 343-353.
[21] M. Ptaszkowska-Koniarz, J. Goscianska and R. Pietrzak, "Adsorption of dyes on the surface of polymer nanocomposites modified with methylamine and copper(II) chloride", *J. Colloid Interface Sci.*, 504 (2017) 549-560.
[22] O. Agboola et al., "A review on polymer nanocomposites and their effective applications in membranes and adsorbents for water treatment and gas separation", *Membranes*, 11(2) (2021) 139.
[23] J. Yimer et al., "Kinetics and equilibrium study of adsorption of phenol red on teff (Eragrostis teff) husk activated carbon", *Int. J. Innov. Sci. Res.*, 11 (2014) 471-476.
[24] A.S. Abouhaswa and T.A. Taha, "Tailoring the optical and dielectric properties of PVC/CuO nanocomposites", *Polym. Bull.*, 77(11) (2020) 6005-6016.
[25] JCPDS 1979, C 29-1133, Joint Committee on Powder Standards, International Center for Diffraction Data, USA (1979).
[26] N.L. My Linh et al., "Phenol red adsorption from aqueous solution on the modified bentonite", *J. Chem.*, 2020(1) (2020) 1504805.
[27] W.L. Danbature et al., "Thermodynamics and kinetics adsorption of phenol red on carbon-CuO nanocomposite", *J. Glob. Ecol. Environ.*, 9(3) (2019) 107-117.
[28] N.T. Joseph et al., "Isotherm and kinetic modeling of adsorption of dyestuffs onto kola nut (Cola acuminata) shell activated carbon", *J. Chem. Technol. Metall.*, 51(2) (2016) ??-??.
[29] A. Mandal, B.B. Dey and S.K. Das, "Thermodynamics, kinetics, and isotherms for phenol removal from wastewater using red mud", *Water Pract. Technol.*, 15(3) (2020) 705-722.
[30] A. Mittal et al., "Adsorption studies on the removal of coloring agent phenol red from wastewater using waste materials as adsorbents", *J. Colloid Interface Sci.*, 337(2) (2009) 345-354.
[31] V.M. Muinde, "Batch adsorption of malachite green from aqueous solutions using low-cost rice husks and synthetic polymer adsorbents: kinetic and equilibrium modelling", PhD diss., University of Nairobi, Kenya (2021).
[32] A. Gholizadeh et al., "Kinetic and isotherm studies of adsorption and biosorption processes in the removal of phenolic compounds from aqueous solutions: comparative study", *J. Environ. Health Sci. Eng.*, 11 (2013) 1-10.
[33] M.A. Malana, R.B. Qureshi and M.N. Ashiq, "Adsorption studies of arsenic on nano aluminium doped manganese copper ferrite polymer (MA, VA, AA) composite: kinetics and mechanism", *Chem. Eng. J.*, 172(2-3) (2011) 721-727.
[34] S. Gamoudi and E. Srasra, "Removal of cationic and anionic dyes using purified and surfactant-modified Tunisian clays: kinetic, isotherm, thermodynamic and adsorption-mechanism studies", *Clay Miner.*, 53(2) (2018) 159-174.
[35] B. Ismail, S.T. Hussain and S. Akram, "Adsorption of methylene blue onto spinel magnesium aluminate nanoparticles: adsorption isotherms, kinetic and thermodynamic studies", *Chem. Eng. J.*, 219 (2013) 395-402.

